ADVANCED THERAPEUTICS
www.advtherap.com

Engineering the Immune Adaptor Protein STING as a Functional Carrier

*Xin Sun, Yun Ni, Yanpu He, Mengdi Yang, Tetsuo Tani, Shunsuke Kitajima, David A. Barbie, and Jiahe Li**

Activation of the stimulator of interferon genes (STING) pathway through cyclic dinucleotides (CDNs) is being explored as potent vaccine adjuvants against infectious diseases and to increase tumor immunogenicity toward cancer immunotherapy. To date, a myriad of synthetic vehicles, including liposomes, polymers, and other nanoparticle platforms, have been developed to improve the bioavailability and therapeutic efficacy of STING agonists in preclinical mouse models. Compared to synthetic materials, protein-based carriers represent an attractive delivery platform owing to their biocompatibility, amenability to genetic engineering, and intrinsic capacity to form well-defined structures. Here, the immune adaptor STING is engineered as aprotein-based delivery system for efficient encapsulation and intracellular delivery of CDNs. Through genetic fusion with a protein transduction domain, the recombinant STING can spontaneously penetrate cells to markedly enhance the delivery of CDNs in a mouse vaccination model and a syngeneic melanoma model. As certain tumor cells can evade immune surveillance via loss of STING expression, authors further unveiled that the STING platform can serve as a functional vehicle to restore the STING signaling in cell lines with impaired STING expression. Altogether, their delivery platform may offer a unique direction toward targeting STING-silenced tumors and augmenting the efficacy of STING-based vaccine adjuvants.

1. Introduction

The cytosolic DNA sensing pathway involving cyclic guanosine monophosphateadenosine monophosphate (GMP-AMP) synthase (cGAS) and the stimulator of interferon (IFN) genes (STING) represents an essential innate immune mechanism in response to foreign pathogens.[1] Upon detection of cytosolic DNA, the intracellular nucleic acid sensor cGAS catalyzes the productions of cyclic dinucleotides (CDNs) such as 2'3'-cyclic GMP-AMP (cGAMP), which functions as a second messenger to bind the adaptor protein STING to initiate type I IFN production and boost dendritic cell (DC) maturation and T cell infiltration.[2] Meanwhile, the cGAS-STING signaling pathway is profound at sensing neoplastic progression by promoting type I IFN production and initiating cytotoxic T cell-mediated antitumor immune response.[3] These fundamental studies have accelerated the development of utilizing synthetic STING agonists to activate the innate and adaptive immune responses as a monotherapy or in combination with immune checkpoint blockade (ICB) for cancer immunotherapy.[4,5]

Despite the promise of CDNs such as cGAMP as immune adjuvants, they suffer from several limitations: 1) CDNs exhibit fast clearance from the injection site, which may induce systemic toxicity, 2) naturally derived CDNs are susceptible to enzymatic degradation, which can lower the efficacy of adjuvanticity potential, and 3) CDNs have inefficient intracellular transport properties due to limited endosomal escape or reliance on the expression of a specific transporter protein.[6–8] To address these challenges, existing efforts are largely focused on two main directions: 1) generation of novel biomaterial-based delivery systems to improve the in vivo delivery of CDNs to activate innate immune cells and 2) discovery of new STING agonist analogs via medicinal chemistry and drug screening to confer greater chemical stability and improved pharmacokinetics.[7–11]

The landscape of STING agonism approaches in cancer immunotherapy have changed in recent years with multiple STING agonists and delivery platforms being evaluated for systemic or local delivery.[7,9] While these approaches mainly target the STING pathway in STING-positive cells in the tumor

Dr. X. Sun, Y. Ni, Dr. Y. He, M. Yang, Prof. J. Li
Department of Bioengineering
Northeastern University
Boston, MA 02115, USA
E-mail: jiah.li@northeastern.edu
Dr. T. Tani, Dr. S. Kitajima, Prof. D. A. Barbie
Department of Medical Oncology
Dana–Farber Cancer Institute
Boston, MA 02215, USA
Dr. S. Kitajima
Department of Cell Biology
Cancer Institute
Japanese Foundation for Cancer Research
Tokyo 135-8550, Japan
Prof. D. A. Barbie
Belfer Center for Applied Cancer Science
Dana–Farber Cancer Institute
Boston, MA 02215, USA

The ORCID identification number(s) for the author(s) of this article can be found under https://doi.org/10.1002/adtp.202100066

DOI: 10.1002/adtp.202100066

microenvironment (TME), such as DCs and stroma cells, it has become increasingly evident that targeting STING in tumor cells is also critical for the therapeutic efficacy of STING-based cancer immunotherapy. However, tumors can exploit multiple escape mechanisms to evade immune recognition and one of the tumor-intrinsic mechanisms is silencing of the expression of STING in cancer cells, for which there is a currently unmet clinical need. Importantly, over the last 5 years, the importance of tumor intrinsic STING has been supported by extensive clinical data in multiple cancers such as melanoma and nonsmall cell lung cancer (NSCLC).[12–14] Therefore, considering the prevalence of STING silencing across various cancers, one limitation of existing STING agonist-based therapeutics is that they cannot activate STING signaling in tumor cells deficient for STING expression.

Here we seek to devise a therapeutic strategy to deliver functional STING protein complexes with cell penetration ability to restore the defective STING signaling in those tumor cells. Previously, we uncovered an unnatural function of a recombinant STING protein that lacks the hydrophobic transmembrane (TM) domain (hereinafter referred to as STINGΔTM).[15] Notably, following delivery via commercial transfection reagents, the STINGΔTM/cGAMP complexes can activate the STING signaling pathway even in cells without endogenous STING expression. In our present work, to bypass the need for any synthetic delivery material, we sought to engineer a protein-based carrier for STING agonists by generating a cell-penetrating STINGΔTM (CP-STINGΔTM) through genetic fusion with a cell-penetrating domain, named Omomyc. As a dominant-negative form of the human *MYC* oncogene, Omomyc was originally identified to target Kirsten rat sarcoma viral oncogene homologue (*KRAS*)-driven tumor cells in several NSCLC xenograft mouse models.[16] Intriguingly, in a synthetic vehicle-free mode, CP-STINGΔTM markedly enhanced delivery of cGAMP in cells, which differ in the levels of endogenous STING expression or cell type. To prove its utility in vivo, we first explored CP-STINGΔTM to enhance the delivery of cGAMP as an adjuvant in a mouse model vaccinated with chicken ovalbumin (OVA).[17] Furthermore, in a syngeneic mouse model of melanoma, we explored a combination immunotherapy regimen consisting of an ICB inhibitor, anti-programmed cell death protein 1 (anti-PD-1), and STING agonism.[18,19] Collectively, our work demonstrated the potential of repurposing the immune sensing receptor as a vehicle to encapsulate and deliver immune adjuvants toward vaccine and cancer immunotherapy development.

2. Results

2.1. Overall Scheme of cGAMP Delivery by CP-STINGΔTM

In contrast to existing delivery strategies such as nanoformulations or synthetic depots to overcome the challenges in encapsulation and intracellular delivery of STING agonist (e.g., cGAMP), we have repurposed the natural receptor STING as a highly modular and simple platform to efficiently bind and deliver cGAMP in vitro and in vivo.[7] Specifically, we took advantage of previous biochemical studies, in which the recombinant C-terminal domain of STING protein (STINGΔTM, 139-379aa for human and 138-378aa for mouse) is known to bind cGAMP with high affinity and stability.[20,21] Additionally, in our previous work, we serendipitously uncovered that the recombinant STINGΔTM could form complexes with cGAMP, and activate the downstream STING signaling following delivery of the complexes by commercial transfection reagents in HEK293T that do not express endogenous STING. On the contrary, recombinant STINGΔTM proteins with catalytically inactive mutations, including S366A and deletion of the last nine amino acids (i.e., ΔC9), failed to activate the STING pathway in HEK293T.[22,23] Building on this serendipitous discovery, to bypass the need for transfection reagents, here we developed a CP-STINGΔTM to deliver cGAMP into different cell types via genetic fusion of a cell-penetrating protein (**Figure 1**a,b). Notably, in contrast to cell-penetrating peptides such as trans-activating transcriptional activator (TAT), we have chosen the Omomyc mini-protein as our cell-penetrating moiety for three reasons: 1) Omomyc (91 amino acids) is derived from a dominant-negative form of the human *MYC* oncogene and has recently shown specific targeting and potent tumor cell penetration capabilities in human cancer cell lines and xenograft mouse models. 2) The natural dimer conformation of Omomyc coincides with STINGΔTM, which also exists as a dimer in the absence of cGAMP. 3) Omomyc may not cause an immunogenicity issue owing to its human origin.[16]

Since the C terminal amino acids of STING directly interact with downstream effector proteins, including TBK1 and IRF3, we genetically fused the cell-penetrating protein Omomyc to the N terminus of STINGΔTM to prevent any steric hindrance posed by Omomyc (Figure 1c). In addition, we generated two essential CP-STINGΔTM mutants to help dissect the mechanisms underlying enhanced delivery of cGAMP: one lacks the effector function to engage with the downstream STING signaling pathway and the other fails to bind cGAMP (**Table 1**).[24–26] In the literature, *E. coli* represents the predominant system to produce the transmembrane-deleted STINGΔTM for various fundamental studies[27–29] and meanwhile Omomyc itself has been successfully produced and characterized for biological functions in *E. coli*.[16,30] For these reasons, we chose *E. coli* to produce our fusion proteins comprising Omomyc and different STINGΔTM variants (Table 1) and purified the 6x Histidine (His) tagged proteins via the metal affinity purification and size exclusion chromatography (SEC). Both size exclusion chromatography studies and sodium dodecyl sulphate-polyacrylamide gel electrophoresis (SDS-PAGE) confirm that the fusion protein can be purified with high yield and homogeneity from *E. coli*. Additionally, the denatured proteins exhibited predicted molecular weights in SDS-PAGE, while the SEC graphs show that CP-STINGΔTM likely forms a tetramer under a native condition in agreement with our previous study (Figure S1a,b, Supporting Information).[15] To confirm the interactions between cGAMP and CP-STINGΔTM, CP-STINGΔTM or the cGAMP-binding deficient mutant CP-STINGΔTM (R237A/Y239A) was titrated with increasing cGAMP concentrations and subject to SEC. As shown Figure S1c,d in the Supporting Information, R237A/Y239A mutations markedly reduced cGAMP binding compared to the wildtype. These preliminary titration experiments also allowed us to prepare the complexes such that CP-STINGΔTM was fully bound to cGAMP for the following in vitro and in vivo studies.

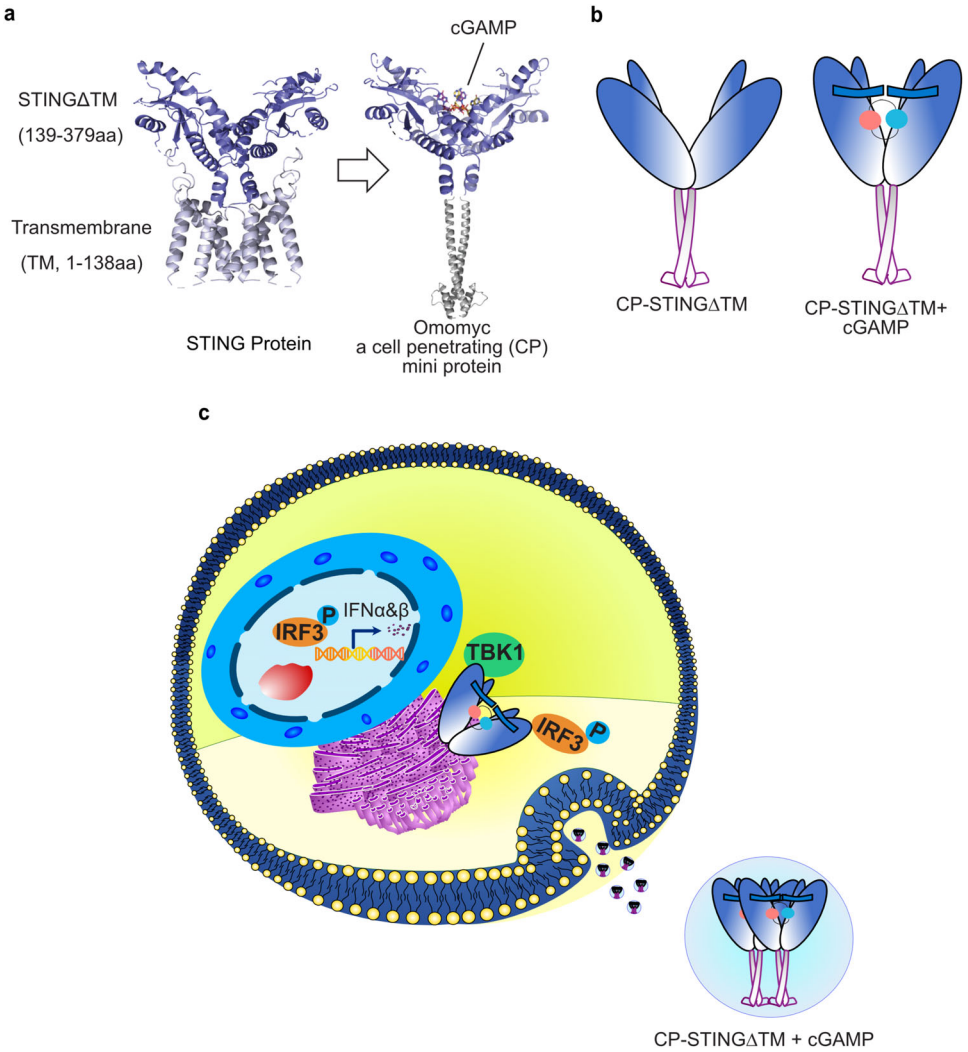

Figure 1. Schematic of using recombinant cell-penetrating (CP)-STINGΔTM as a biologically functional platform for cGAMP delivery. a) To bypass the need for synthetic vehicles, we designed and engineered a CP-STINGΔTM by replacing the transmembrane (TM) of the full-length STING with Omomyc, a cell-penetrating mini protein. b) A cartoon model illustrating how CP-STINGΔTM binds cGAMP. c) By fusing with the cell-penetrating domain, the CP-STINGΔTM is capable of penetrating cells, delivering cGAMP, and engaging with downstream proteins such as tank-binding kinase 1 (TBK1) and IFN regulatory factor 3 (IRF3), which result in the production of type I IFNs.

2.2. CP-STINGΔTM Can Effectively Penetrate Cells

While Omomyc protein itself has been shown to penetrate different lung cancer cell lines in vitro as well as in mouse lung xenografts, it remains to be investigated whether genetic fusion of Omomyc with STINGΔTM can indeed penetrate cells spontaneously. We first characterized physiochemical properties of CP-STINGΔTM proteins alone or in complexed with cGAMP in vitro through SEC and dynamic light scattering (DLS). Our SEC results indicated that CP-STINGΔTM can complex with cGAMP (Figure S1c,d, Supporting Information). In addition, the proteins alone or protein complexes exhibited an average size of 10 nm in diameter, and were stable at room temperature for up to 96 h in phosphate-buffered saline (PBS) (Figures S11 and S12, Supporting Information). To assess the cell-penetrating potential of CP-STINGΔTM, we treated two human NSCLC cell lines with

Table 1. STING variants used in this study.

STING variants[a)]	Description
STINGΔTM	STING lacking the N terminal transmembrane domain
STINGΔTMΔC9	9-Amino acid deletion at the C terminus that abolishes type 1 IFN induction
STINGΔTM(R238A/Y240A)	Deficient for cGAMP binding
CP-STINGΔTM	Inclusion of a cell-penetrating domain named Omomyc to bypass transfection reagent
CP-STINGΔTMΔC9	
CP-STINGΔTM(R238A/Y240A)	
CP-STINGΔTM-dsred	

[a)] Amino acid positions represent the human STING (1-379aa), which are conserved in the mouse STING (1-378aa).

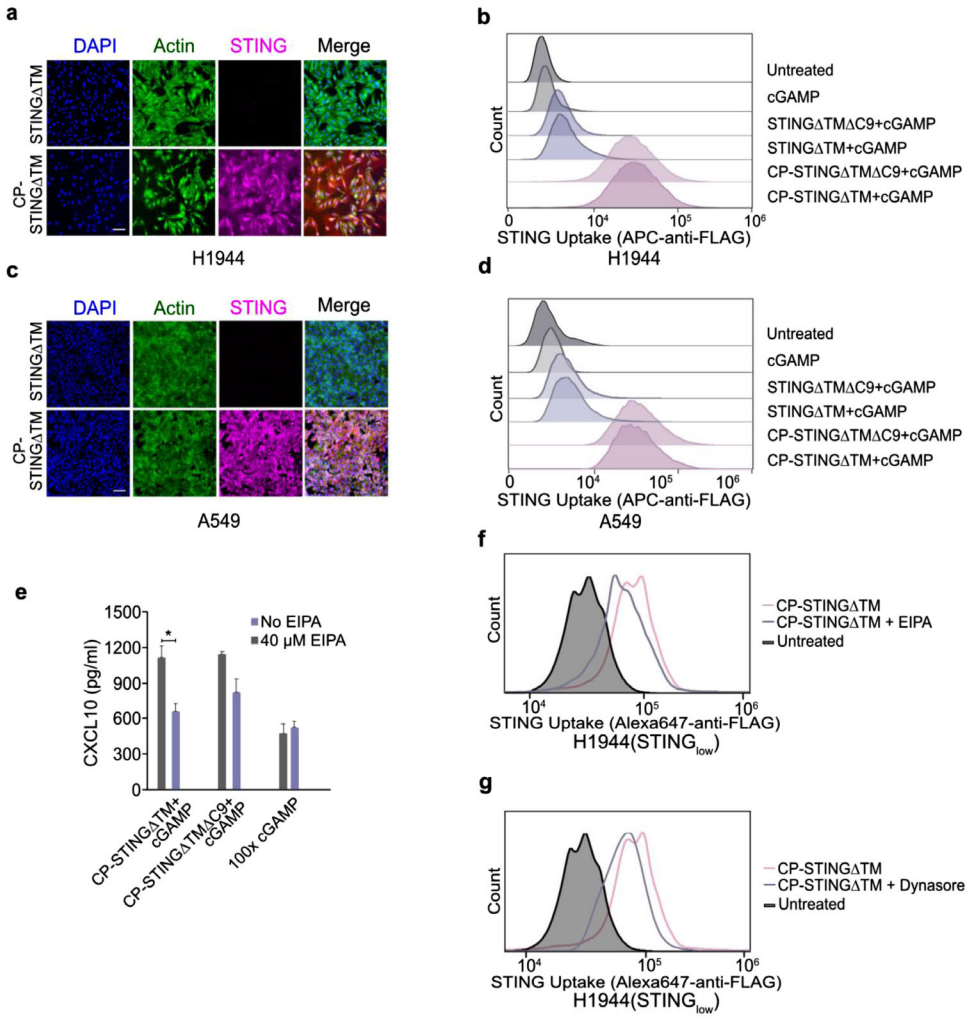

Figure 2. CP-STINGΔTM proteins are internalized by cancer cells. Fluorescence microscopy imaging of internalized CP-STINGΔTM in a) H1944 ($STING_{low}$) with downregulated STING expression and c) A549 ($STING_{absent}$) without any STING expression (scale bar = 100 μm). Flow cytometry of internalized CP-STINGΔTM in b) H1944 ($STING_{low}$) with downregulated STING expression and d) A549 ($STING_{absent}$) without any STING expression. Cells were treated with "40 μg mL^{-1} CP-STINGΔTM" + 1 μg mL^{-1} cGAMP" or "40 μg mL^{-1} STINGΔTM + 1 μg mL^{-1} cGAMP" for 24 h before staining with APC-anti-FLAG. e) H1944($STING_{low}$) were preincubated with 40 × 10^{-6} M EIPA for 2 h and treated with "40 μg mL^{-1} CP-STINGΔTM + 1 μg mL^{-1} cGAMP" or "40 μg mL^{-1} STINGΔTM + 1 μg mL^{-1} cGAMP" or 100 μg mL^{-1} cGAMP, CXCL10 production was inhibited by macropinocytosis inhibitor EIPA. Representative flow cytometry analysis of CP-STINGΔTM uptake in H1944 pretreated with indicated inhibitors targeting f) macropinocytosis and g) endocytosis, respectively.

low or absent STING, H1944 and A549,[14] for 24 h followed by immunostaining against an 8-amino acid FLAG epitope (DYKDDDDK) encoded in between Omomyc and STINGΔTM. Because the FLAG epitope is not known to be expressed by mammalian cells, we could make use of anti-FLAG staining to distinguish exogenously delivered STING protein variants from endogenous STING proteins. Moreover, in contrast to covalently conjugating proteins with fluorescent dyes, which typically modify the surface amine or cysteine groups of proteins, our approach can prevent altering the pharmacokinetics of intracellular protein accumulation. As shown in **Figure 2**a,c, CP-STINGΔTM exhibited efficient intracellular uptake in H1944 and A549, while STINGΔTM alone failed to penetrate cells owing to the lack of Omomyc to promote cell penetration. In addition, we also genetically fused Omomyc to the catalytically inactive mutant STINGΔTMΔC9, which is known to abolish STING function due to the deletion of 9 amino acids at the very C terminus. As shown in Figure S2a,c,e in the Supporting Information, CP-STINGΔTMΔC9 showed comparable degrees of internalization, which confirmed that the intracellular uptake is mediated by Omomyc instead of STING. To further corroborate our findings beyond fluorescence microscopy, we performed flow cytometry to confirm the uptake profiles of different STING variants after intracellular staining against the same synthetic epitope FLAG (Figure 2b,d). In addition to the NSCLC cell lines, we validated the uptake of CP-STINGΔTM and CP-STINGΔTMΔC9 in human melanoma and ovarian cancer cell lines by fluorescence microscopy and flow cytometry (Figure S2b,d,e, Supporting Information). Finally, to dissect the mechanism by which the cell-penetrating STINGΔTM enters cells, we tested a range of small molecule

inhibitors targeting different endocytic pathways including: 5-(*N*-ethyl-*N*-isopropyl) amiloride (EIPA), chlorpromazine, Dynasore, cyclodextrin, and Filipin. Among the small molecule inhibitors we have tested, a macropinocytosis inhibitor, EIPA and an endocytosis inhibitor, Dynasore exhibited a dose-dependent inhibition of CP-STINGΔTM in H1944 (Figure 2e–g and Figure S2f,g, Supporting Information).[16,31] In contrast, inhibitors targeting other uptake pathways failed to inhibit the uptake of CP-STINGΔTM (Figure S2h,i, Supporting Information). Of note, our findings agree with the previous work, in which the Omomyc protein itself was taken up by cancer cells primarily through the macropinocytosis and endocytosis pathways.[16] Therefore, we conclude that the cell-penetrating capability of the fusion protein is mediated by Omomyc in a macropinocytosis and endocytosis-dependent manner.

2.3. CP-STINGΔTM Enhances cGAMP Delivery and STING Activation in a Panel of Lung and Melanoma Cell Lines with Impaired STING Expression

In contrast to innate immune cells, which are highly sensitive to cGAMP-mediated STING activation, previous work by others have shown that downregulation of STING in tumor cells greatly reduced the sensitivity of cancer cells to STING agonists, which can promote immune suppression and exclusion of cytotoxic T cells in the TME.[12,14] Therefore, we sought to ask whether the fusion protein could promote intracellular delivery of the STING agonist cGAMP in a panel of cell lines with reduced sensitivity to STING agonists. We first focused on two $STING_{low}$ NSCLC cell lines, H1944 and H2122, in which the expression of endogenous STING is downregulated due to histone methylation at the native STING promoter.[14] As shown in **Figure 3**a and Figure S3c in the Supporting Information, we compared "CP-STINGΔTM + cGAMP," "CP-STINGΔTMΔC9 + cGAMP," free cGAMP, and lipofectamine-transfected cGAMP to vehicle control-treated cells. Of note, a 1:1 molar ratio of one STING dimer to one cGAMP was prepared for different STING/cGAMP complexes. Impressively, the codelivery systems comprising "CP-STINGΔTM + cGAMP" or "CP-STINGΔTMΔC9 + cGAMP" required ≈100-fold lower concentration of cGAMP than free cGAMP or lipofectamine-transfected cGAMP to induce comparable levels of CXCL10, one of the chemokines that can be induced by the STING pathway.[32,33] In addition, since the STING activation in tumor cells can upregulate major histocompatibility complex I (MHC-I) to promote cytotoxic T cell recognition, we measured the surface expression of MHC-I in the same cancer cells.[34] Consistent with measurement of CXCL10 by enzyme-linked immunosorbent assay (ELISA), "CP-STINGΔTM + cGAMP" and "CP-STINGΔTMΔC9 + cGAMP" similarly enhanced surface expression of MHC class I in H1944 and melanoma cells (Figure S3d,e, Supporting Information).

To explain our findings, we first ruled out the possibility of endotoxin contamination resulting from protein purification from *E. coli*, as CP-STINGΔTM or CP-STINGΔTMΔC9 protein alone of equivalent concentrations did not induce CXCL10 (Figure 3a). It is intriguing, however, delivery of cGAMP by the catalytically inactive CP-STINGΔTMΔC9, in which the interaction of STING with TBK1 and IRF3 is disabled, enhanced the STING activation to a degree similar to that of the wildtype (i.e., CP-STINGΔTM) (Figure 3a). We hypothesized that in the $STING_{low}$ cell lines H1944 and H2122, the CP-STINGΔTM primarily may serve as a chaperon by promoting delivery of cGAMP into tumor cells. To test this hypothesis, we generated two additional fusion proteins: CP-dsRed and CP-STINGΔTM (R238A/Y240A). Importantly mutations of the 238th arginine (R238) and 240th tyrosine (Y240) to alanine (A) are known to abolish the ability of STING to bind cGAMP.[26] As shown in Figure 3a and Figure S3d,e in the Supporting Information, these two protein variants failed to enhance CXCL10 production to the same extent as "CP-STINGΔTM + cGAMP" and "CP-STINGΔTMΔC9 + cGAMP." Therefore, through genetic mutations that inactivate two separate functions of STING, including the effector and cGAMP-binding capabilities, we have found that in $STING_{low}$ cells, CP-STINGΔTM primarily act as a chaperon to efficiently deliver cGAMP intracellularly and therefore greatly enhancing the STING activation.

Since cGAMP exhibits high binding affinity to STING, how cGAMP unbound and bond to the native STING from tumor cells remained to be understood. Since endogenous STING has been shown to undergo lysosomal degradation within a few hours upon activation by STING agonists,[35] we hypothesized that recombinant STING proteins are also degradable inside cells in part through the protein turnover pathway involving lysosomes inside cells. To test the hypothesis, we treated B16F10 cells with CP-STINGΔTM + cGAMP in the absence or presence of a lysosomal inhibitor, chloroquine (CQ). Since the epitope FLAG was inserted between Omomyc and STINGΔTM, the degree of anti-FLAG staining would reflect the integrity of the fusion proteins. Thus, we used anti-FLAG as a proxy to assess the intracellular degradation of CP-STINGΔTM by flow cytometry. While the majority of CP-STINGΔTM degraded over 48 h in the absence of CQ, concurrent treatment of CQ markedly slowed down the degradation of CP-STINGΔTM at 24 and 48 h timepoints (Figure S9, Supporting Information).

Motivated by the ability of CP-STINGΔTM to markedly enhance cGAMP delivery and STING activation in $STING_{low}$ cells, we further extended our observations to A549 (human NSCLC) and SK-MEL-5 (human melanoma), which do not express endogenous STING ($STING_{absent}$).[14,36] Interestingly, we found that only "CP-STINGΔTM + cGAMP" induced CXCL10, while the catalytically inactive CP-STINGΔTMΔC9 along with cGAMP did not (Figure 3b). Additionally, "STINGΔTM + cGAMP" failed to induce CXCL10, which can be explained by the absence of Omomyc to facilitate cell penetration (Figure 3a). These observations imply that codelivery of CP-STINGΔTM and cGAMP functionally restored the deficient STING signaling in $STING_{absent}$ cells. To further confirm this hypothesis, we utilized Clustered Regularly Interspaced Short Palindromic Repeats (CRISPR) to genetically knock out endogenous cGAS and STING, respectively, in H1944. Notably, the cGAS knockout is known to inhibit the production of endogenous cGAMP.[37] Consistent with data in $STING_{low}$ cell lines, in H1944 with cGAS knockout but intact STING, both "CP-STINGΔTM + cGAMP" and "CP-STINGΔTMΔC9 + cGAMP" could comparably induce CXCL10 expression, suggesting that endogenous cGAMP is not required for the activation of STING signaling (Figure S3f, Supporting Information). In H1944 with only STING

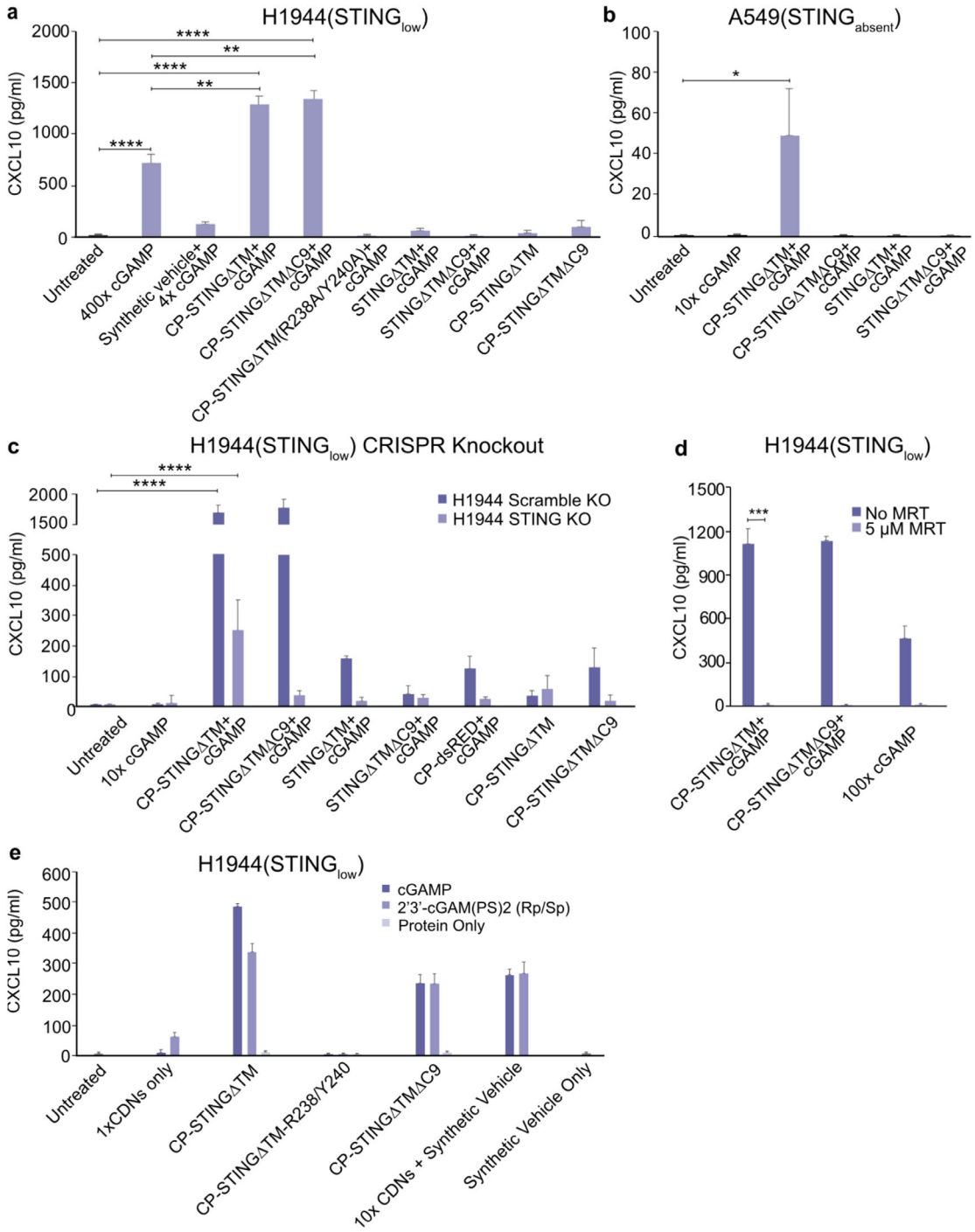

Figure 3. CP-STINGΔTM markedly enhances cGAMP delivery and STING activation in cancer cell lines with impaired STING expression. a) CP-STINGΔTM plays a chaperon role in H1994 (STING$_{low}$) that have downregulated STING expression. Specifically, CXCL10 was remarkably enhanced by "10 μg mL^{-1} CP-STINGΔTM + 0.25 μg mL^{-1} cGAMP" or "10 μg mL^{-1} CP-STINGΔTMΔC9 (catalytically inactive mutant) + 0.25 μg mL^{-1} cGAMP" compared to 100–400-fold higher concentration of free cGAMP and 40-fold higher concentration of cGAMP delivered by Lipofectamine 2000. b) "CP-STINGΔTM + cGAMP" forms a functional complex in A549 (STING$_{absent}$), which does not express endogenous STING. Only "40 μg mL^{-1} CP-STINGΔTM + 1 μg mL^{-1} cGAMP" could induce CXCL10. c) After knocking out endogenous STING in H1944 by CRISPR, CXCL10 expression was only induced by "40 μg mL^{-1} CP-STINGΔTM + 1 μg mL^{-1} cGAMP" but not by the catalytic inactive "40 μg mL^{-1} CP-STINGΔTMΔC9 + 1 μg mL^{-1} cGAMP" or free cGAMP. d) The CXCL10 production was inhibited by the TBK1 inhibitor—MRT, which indicates that the enhanced STING signaling by CP-STINGΔTM or CP-STINGΔTMΔC9 was dependent on the TBK1, a key component in the STING pathway. e) Codelivery of CP-STINGΔTM and a synthetic, nondegradable cGAMP analog, cGAMP(PS)$_2$(Rp/Sp), also enhances CXCL10 production in comparison to free cGAMP(PS)$_2$(Rp/Sp) or 10x cGAMP(PS)$_2$(Rp/Sp) transfected by Lipofectamine 2000, which suggests that CP-STINGΔTM promotes the cGAMP delivery instead of protecting cGAMP from enzymatic degradation. *P < 0.05, **P < 0.01, ***P < 0.001, ****P < 0.0001. Values = mean ± SEM (standard error of the mean), n = 4.

knockout, however, CXCL10 expression was induced by "CP-STINGΔTM + cGAMP" but not the catalytically inactive "CP-STINGΔTMΔC9 + cGAMP" (Figure 3c), which is consistent with findings in A549 and SK-MEL-5 cells, in which endogenous STING expression is completely absent (Figure 3b and Figure S3f, Supporting Information). In addition, concurrent treatment with a TBK1 inhibitor, MRT, repressed the production of CXCL10 in the cells treated with "CP-STINGΔTM + cGAMP" and "CP-STINGΔTMΔC9 + cGAMP" (Figure 3d).[15] Therefore, through both genetic and pharmacological inhibition of key proteins in the STING pathway, we have shown that "CP-STINGΔTM + cGAMP" acts as a functional complex to induce STING signaling in the cells lacking endogenous STING expression. Finally, since cGAMP can be degraded by Ectonucleotide pyrophosphatase/phosphodiesterase 1 (ENPP1), which is abundant in extracellular and intracellular environments, another possibility for enhanced cGAMP delivery is that CP-STINGΔTM may protect cGAMP from ENPP1-mediated hydrolysis.[8] To test this possibility, we explored $cGAM(PS)_2(Rp/Sp)$, a synthetic nondegradable cGAMP analog, in H1944, and observed that "CP-STINGΔTM + $cGAM(PS)_2(Rp/Sp)$" and "CP-STINGΔTMΔC9 + $cGAM(PS)_2(Rp/Sp)$," markedly enhanced CXCL10 production in comparison to $cGAM(PS)_2(Rp/Sp)$ alone of equivalent concentration or at a 10x concentration transfected by a commercial transfection reagent. Moreover, CP-STINGΔTM (R238A/Y240A), in which the two mutations R238A and Y240A abolish the cGAMP binding, failed to enhance CXCL10 production in the codelivery with $cGAM(PS)_2(Rp/Sp)$ (Figure 3e).

2.4. CP-STINGΔTM Enhances the Adjuvanticity Potential of cGAMP

cGAMP has been explored as a potent vaccine adjuvant that promotes both humoral and cellular immune responses in different mouse vaccination models.[38] However, free cGAMP is prone to fast clearance and degradation owing to low molecular weight (≈600 Da) and the presence of hydrolyzable phosphoester bonds, respectively. To address these limitations, a myriad of synthetic biomaterials have been developed to enhance the delivery efficacy of cGAMP. In our own work, motivated by enhanced activation of the STING pathway by CP-STINGΔTM in different cell types, we ask whether it could serve as a protein-based delivery platform to efficiently deliver cGAMP as an immune adjuvant. To this end, we made use of the murine dendritic cell line DC 2.4 as a model of antigen-presenting cells (APCs).[7] Similar to our findings in cancer cells, it was shown that CP-STINGΔTM + cGAMP greatly induced expression of CXCL10 and surface expression of MHC-I compared to free cGAMP (**Figure 4**a,b). In addition to measuring CXCL10, we also used the RAW ISG, a reporter cell line for the STING pathway.[15] As shown in Figure S10 in the Supporting Information, both "CP-STINGΔTM + cGAMP" and "CP-STINGΔTMΔC9 + cGAMP" enhanced the induction of interferons in comparison to 10x concentrated free cGAMP via the RAW blue assay. Similar to DC 2.4, because RAW ISG cells express endogenous STING, CP-STINGΔTM acted as a chaperon in this setting.

Next, we explored CP-STINGΔTM as a carrier for STING-based immune adjuvants. To this end, wild-type C57BL/6 mice were vaccinated with endotoxin-free chicken OVA (Figure S13, Supporting Information), along with free cGAMP or cGAMP + CP-STINGΔTM serving as an immune adjuvant.[15] Following a priming-boost protocol with a 2-week interval, we quantified the levels of OVA-specific total immunoglobulin G (IgG) as well as type I IFN-associated IgG2c from mouse serum, of which the latter IgG subtype can be induced through activation of the STING pathway. As shown by the OVA-specific ELISA, the "OVA + cGAMP + CP-STINGΔTM" treatment group increased the levels of OVA-specific IgG and IgG2c by nearly tenfold compared to "OVA + cGAMP + CP-STINGΔTM (R237A/Y239A)," "OVA + cGAMP + STINGΔTM," and "OVA + cGAMP" (Figure 4b,c and Figure S4a, Supporting Information). In addition to analyzing antibody responses, the activation of STING pathway can also boost the cellular immunity, which is critical for immune clearance of tumor cells and intracellular pathogens.[39] Therefore, in the same cohort of mice, we measured the percentage of CD8 T cells carrying the MHC-I-SIINFEKL epitope ($OVA_{257\text{-}264aa}$) via tetramer staining (Figure S4b and Figure S8, Supporting Information). In agreement with studies in humoral responses, "OVA + cGAMP + CP-STINGΔTM" exhibited the highest induction of SIINFEKL-specific CD8 T cells among different treatment groups. Furthermore, when comparing CP-STINGΔTM to STINGΔTM, the latter of which does not have the cell-penetrating protein domain, CP-STINGΔTM markedly enhanced OVA-specific IgG and IgG2c as well as SIINFEKL-restricted CD8 T cells (Figure 4b,c and Figure S4b, Supporting Information).[40] We reasoned that it is due to increased retention and intracellular uptake mediated by the cell-penetrating protein Omomyc. Indeed, in a later experiment, we found that CP-STINGΔTM exhibited greater retention in tumors than STINGΔTM at 96 h post injection (Figure 6a,b). Next, we made use of the same cohort of vaccinated C57BL/6 mice to examine whether the increased induction in antigen-specific IgG and CD8 levels could confer greater protection in a prophylactic syngeneic mouse melanoma model. Specifically, 1 week after the boost, we challenged the mice with B16 melanoma cells engineered to express the SIINFEKL epitope. As shown in Figure 4d,e, the cohort vaccinated with "OVA + cGAMP + CP-STINGΔTM" combination displayed the slowest tumor growth rates and longest survival rates.

2.5. Codelivery of CP-STINGΔTM and cGAMP Augments Tumor Cell Killing by Antigen-Specific T Cells Ex Vivo

In addition to promoting maturation and crosspresentation of dendritic cells for T cell priming, which serves as the very first step of immune clearance of tumor cells, activation of the STING pathway in tumor cells has been shown to augment cytotoxic T cell-mediated cancer cell killing by upregulating MHC-I on the surface of tumor cells.[34] Motivated by the aforementioned vaccination and prophylactic mouse model studies, we next explored whether CP-STINGΔTM and cGAMP can enhance tumor cell killing. To this end, in an ex vivo model, we generated two isogenic B16 melanoma cell lines expressing either chicken ovalbumin peptide OVA 257–264 (SIINFEKL)-green fluorescence protein (GFP) fusion or GFP alone and treated them with free cGAMP,

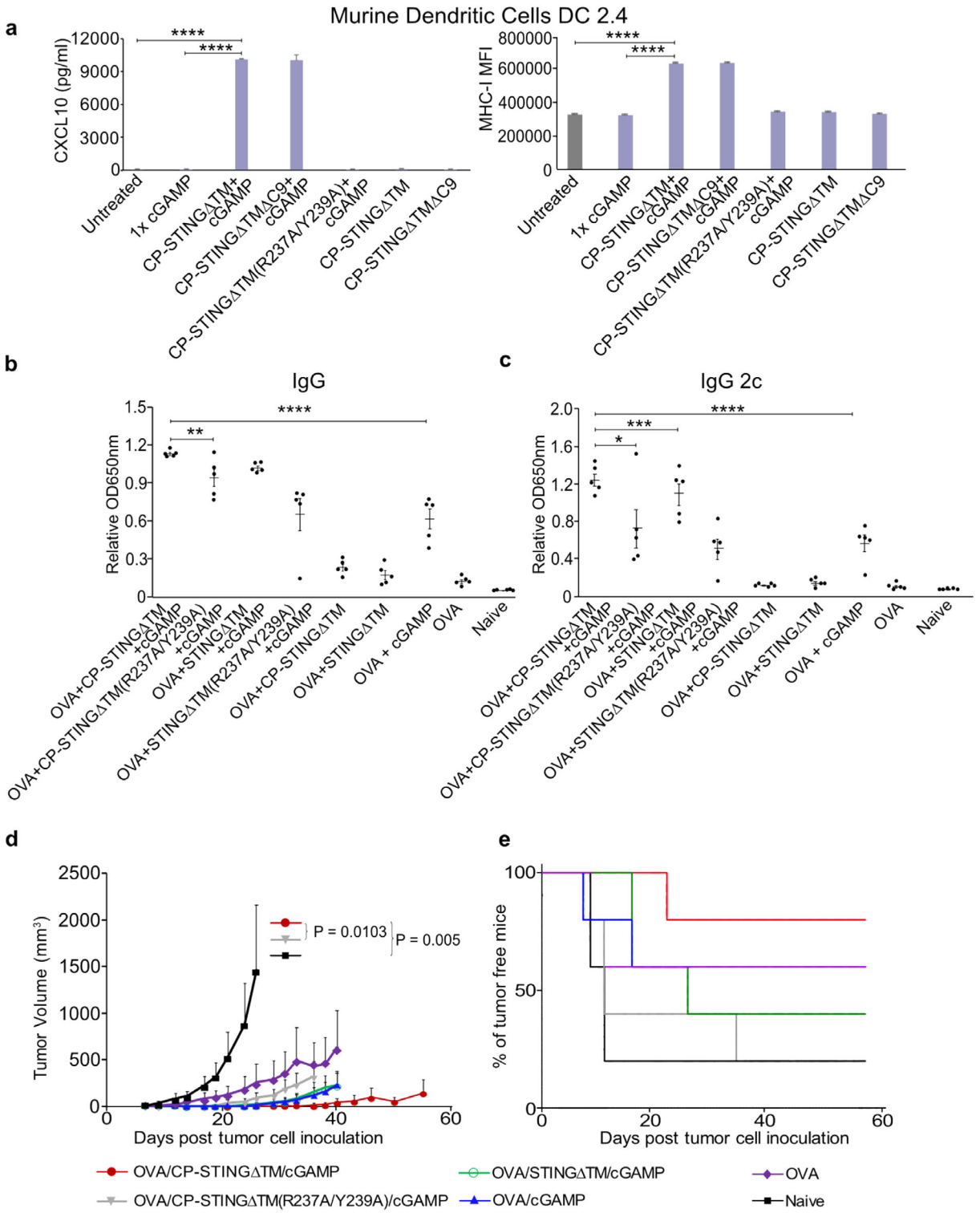

Figure 4. CP-STINGΔTM enhances the adjuvanticity potential of cGAMP for vaccination and prophylactic tumor models. a) In murine dendritic cells DC 2.4, "40 μg mL^{-1} CP-STINGΔTM + 1 μg mL^{-1} cGAMP" markedly induced CXCL10 expression as evidenced by ELISA as well as upregulated surface expression of MHC-I measured by flow cytometry. Levels of b) OVA-specific total IgG and c) the type I IFN-associated subtype IgG2c in groups of C57BL/6 mice ($n = 5$). Mice were immunized with OVA alone or OVA mixed with 1 μg mL^{-1} free cGAMP or combinations of 40 μg mL^{-1} STINGΔTM variants with or without 1 μg mL^{-1} cGAMP on days 0 and 14 via tail-based injection. On days 21, sera from different vaccination combinations were collected for OVA-specific total IgG and IgG2c quantification. On day 21, the same cohort of mice were challenged with 1 million B16-OVA (257-264aa) subcutaneously. d) Overall tumor growth and e) survival rates were shown ($N = 5$ per treatment group). Values are reported as mean ± SEM ($N = 5$). Statistical analysis was performed by one-way analysis of variance (ANOVA) according to the scales of $^*P < 0.05$, $^{**}P < 0.01$, $^{***}P < 0.001$, and $^{****}P < 0.0001$.

"cGAMP + CP-STINGΔTM," "cGAMP + CP-STINGΔTMΔC9," and "cGAMP + CP-STINGΔTM (R237/Y239A)" for 48 h.[41] After the supernatant was removed from the tumor cells, carboxyfluorescein succinimidyl ester (CFSE)-stained SIINFEKL-specific CD8 T cells, which were harvested from lymph nodes of OT-1 mice, were cocultured with tumor cells (**Figure 5**a). It is noteworthy that by pretreating tumor cells with cGAMP and different STING protein variants followed by washing and coculturing with antigen-specific T cells, we specifically tested the effects of STING activation in tumor cells. As shown in Figure 5b,c, following a 120 h coculture, cGAMP complexed with CP-STINGΔTM and CP-STINGΔTMΔC9 induced the highest T cell proliferation as evidenced by T cell division-mediated CFSE dilution in flow cytometry. Moreover, the highest efficacy of tumor killing was detected in the same treatment groups by staining viable tumor cells with 3-(4,5-dimethylthiazol-2-yl)-2,5-diphenyltetrazolium bromide (MTT) after washing away nonadherent T cells (Figure 5d). Of note, the tumor killing was only detectable in B16 cells bearing the SIINFEKL epitope but not in the GFP-expressing B16 cells in the coculture with OT-1 cells, indicating that the increased T cell proliferation and tumor cell killing were antigen-specific (Figure S5a,b, Supporting Information). To confirm that the increased T cell proliferation and killing resulted from enhanced tumor cell recognition by OT-1 T cells, after treating SIINFEKL-expressing B16 with cGAMP and different STING variants for 48 h, we quantified the expression levels of MHC-I and SIINFEKL-restricted MHC-I on the surface of tumor cells by flow cytometry. As shown in Figure 5e and Figure S5c in the Supporting Information, only "CP-STINGΔTM + cGAMP" and "CP-STINGΔTMΔC9 + cGAMP" markedly upregulated the expression of MHC-I and SIINFEKL-restricted MHC-I in comparison to free cGAMP and other control treatment groups. We reason that since B16 cells express endogenous STING (Figure S3a, Supporting Information), CP-STINGΔTM acted as a chaperon to enhance cGAMP delivery into tumor cells in this setting.

2.6. Codelivery of CP-STINGΔTM and cGAMP Enhances the Therapeutic Efficacy of ICB

Having validated the enhanced tumor cell killing by OT-1 cells via codelivery of CP-STINGΔTM and cGAMP ex vivo, we further examined whether this approach could augment the efficacy of the combination immunotherapy involving STING agonism and ICB. Here, we made use of an immunogenic mouse melanoma cancer model bearing YUMMER1.7 tumor cells for three reasons: First, YUMMER1.7 cells carry *Braf* mutation and *Pten* loss that mimic the most frequent mutations happening in melanoma patients.[42] Second, tumors with increased immunogenicities are generally responsive to ICB, such as anti-PD-(L)1, among which lung cancer and melanoma are of high mutation burden.[43] Third, STING activation in the TME has been shown to improve the therapeutic efficacy of ICB in different syngeneic mouse cancer models.[44]

Before the treatment study, we first confirmed that CP-STINGΔTM can be internalized by tumor cells and other cell types in the TME. Specifically, when YUMMER1.7 tumors reached ≈150 mm^3 in C57BL/6 mice, a single dose of CP-STINGΔTM was administered intratumorally. Mice were sacrificed at 96 h and tumors were harvested for cryosectioning and immunostaining using the anti-FLAG antibody specific for recombinant STING protein variants. As shown in **Figure 6**a, CP-STINGΔTM but not STINGΔTM was readily detectable across different tumor slices in a homogeneous pattern at 96 h after a single intratumoral (i.t.) administration, and CP-STINGΔTM was primarily localized in the cytoplasm, suggesting that the presence of the cell-penetrating domain Omomyc domain facilitated the retention of recombinant STING in the TME. To corroborate this finding, in a separate cohort of mice, single cells were prepared for intracellular staining against the same FLAG epitope. Similar to our in vitro cellular uptake studies, CP-STINGΔTM efficiently penetrated tumor cells in comparison to STINGΔTM that lacks the cell-penetrating capability (Figure 6b).

Next, we investigated the therapeutic efficacy of CP-STINGΔTM and cGAMP in combination with anti-PD1 in the Yummer1.7 syngeneic mouse model (Figure 6c). Of note, we initiated treatment in mice with relatively large subcutaneous tumors, which are more challenging to treat with immunotherapy than smaller tumors.[7] After tumors reached 150–170 mm^3, CP-STINGΔTM, CP-STINGΔTMΔC9, CP-STINGΔTM(R237A/Y239A), and STINGΔTM were intratumorally administered with cGAMP, while anti-PD1 was given intraperitoneally at optimized doses every 2 d for a total of four treatments (Figure 6c). Over the duration of treatment, no significant weight loss was detected among different treatment groups in comparison to the vehicle control group (Figure S6a, Supporting Information). Importantly, both CP-STINGΔTM and CP-STINGΔTMΔC9 showed marked reduction in the tumor progression compared to CP-STINGΔTM(R237A/Y239A) and STINGΔTM treatment groups (Figure 6d,e). These findings agree with our studies in vitro: 1) The mutations R237A/Y239A in STING abolish the binding of cGAMP, and therefore CP-STINGΔTM(R237A/Y239A) cannot effectively deliver cGAMP into target cells. 2) STINGΔTM alone cannot efficiently penetrate target cells due to the absence of the Omomyc protein. 3) Because cancer cells and hematopoietic cells in tumors express endogenous STING, CP-STINGΔTM plays a chaperon role in enhancing the intracellular delivery of cGAMP such that there was no detectable difference between CP-STINGΔTM and CP-STINGΔTMΔC9, the latter of which cannot activate the STING signaling. In addition to tumor volume therapeutic efficacy, we further measured proinflammatory cytokines in a separate cohort of mice bearing the same tumor cells.[45] The treatment group of "CP-STINGΔTM + cGAMP" displayed increased expression of tumor necrosis factor (TNF)α, IFNγ, and CXCL10 in comparison to "STINGΔTM + cGAMP" and the untreated group (Figure 6f,g and Figure S6b, Supporting Information).

3. Discussion

In this study, we have successfully developed a protein carrier (CP-STINGΔTM) for efficient cytosolic delivery of STING agonists by merging the inherent capacity of the transmembrane deleted STING (STINGΔTM) in binding cGAMP and activating the downstream STING signaling with the CP miniprotein Omomyc, the latter of which was recently validated in several

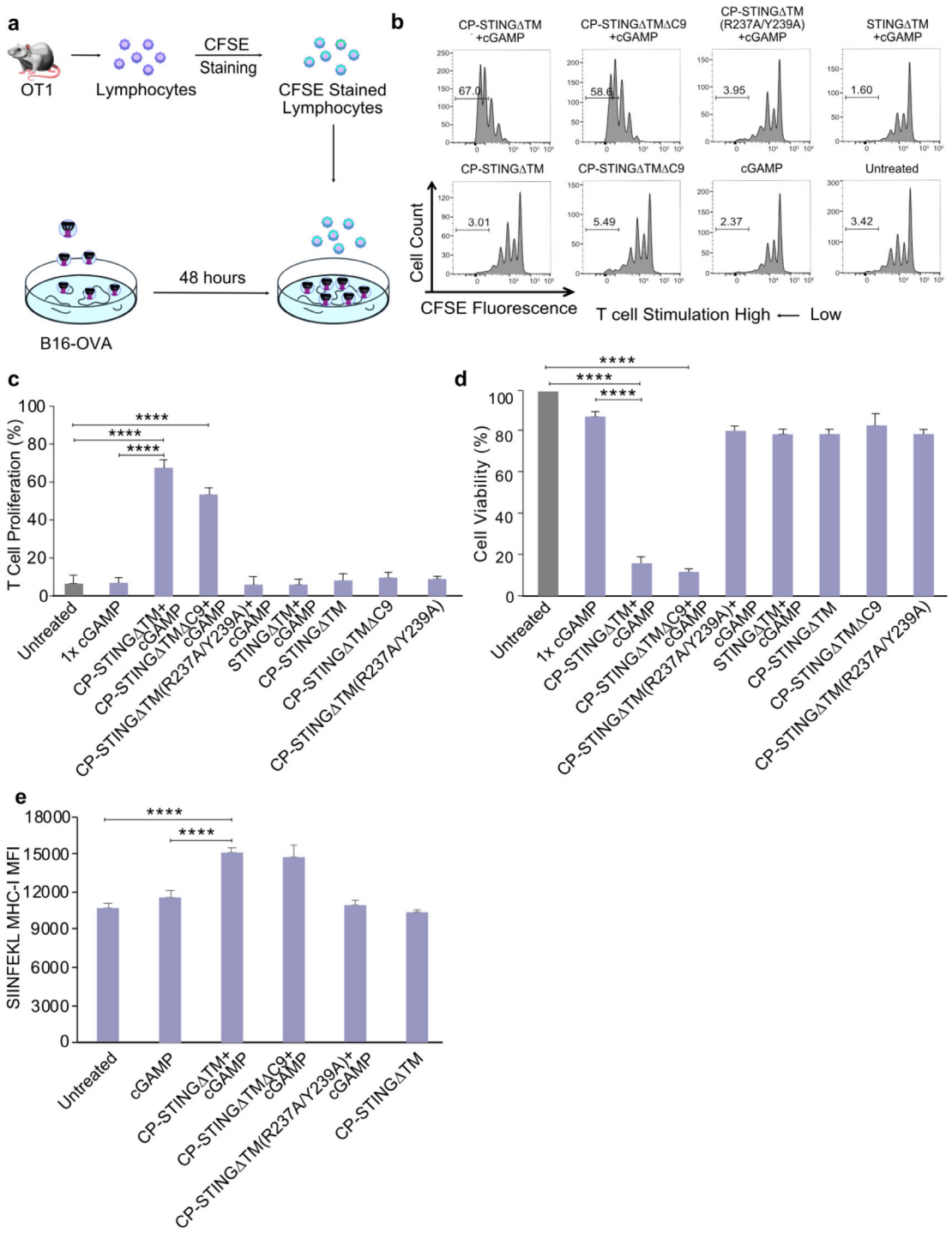

Figure 5. *Ex vivo* T cell-mediated cancer cell killing after activating the STING pathway in tumor cells. a) CFSE-labeled OT1 cells were added into B16-OVA (257-264aa, SIINFEKL) cells that were pretreated with cGAMP plus indicated STINGΔTM variants for 48 h (≈10:1 ratio of effector T cell to tumor cells). Proliferated T cells were assayed 5 d later. b) Representative CFSE flow cytometry data from one of four independent experiments are displayed. c) Quantification of T cell proliferation by CFSE staining. While the pretreatment groups "CP-STINGΔTM + cGAMP" and "CP-STINGΔTMΔC9 + cGAMP" promoted T cell proliferation, the variants with deficiency in cGAMP binding or cell penetration did not. d) OT1-mediated cancer cell killing. B16-OVA (257-264aa, SIINFEKL) that had been pretreated with indicated STING variants plus cGAMP for 48 h were cocultured with OT1 cells. After 5 d, nonadherence T cells were removed by washing and the viability of adherent tumor cells was assessed by the MTT assay. Experiments were representative of three biological replicates. e) Upregulation of SIINFEKL-restricted MHC-I on the surface of B16-OVA (257-264aa). After treating tumor cells with cGAMP plus different STING variants for 48 h, only "CP-STINGΔTM + cGAMP" and "CP-STINGΔTMΔC9 + cGAMP" upregulated the expression of SIINFEKL-restricted MHC-I. Graphs are expressed as mean ± SEM ($n = 4$) and statistical analysis by one-way ANOVA according to the following scale: $^{*}P < 0.05$, $^{**}P < 0.01$, $^{***}P < 0.001$, and $^{****}P < 0.0001$.

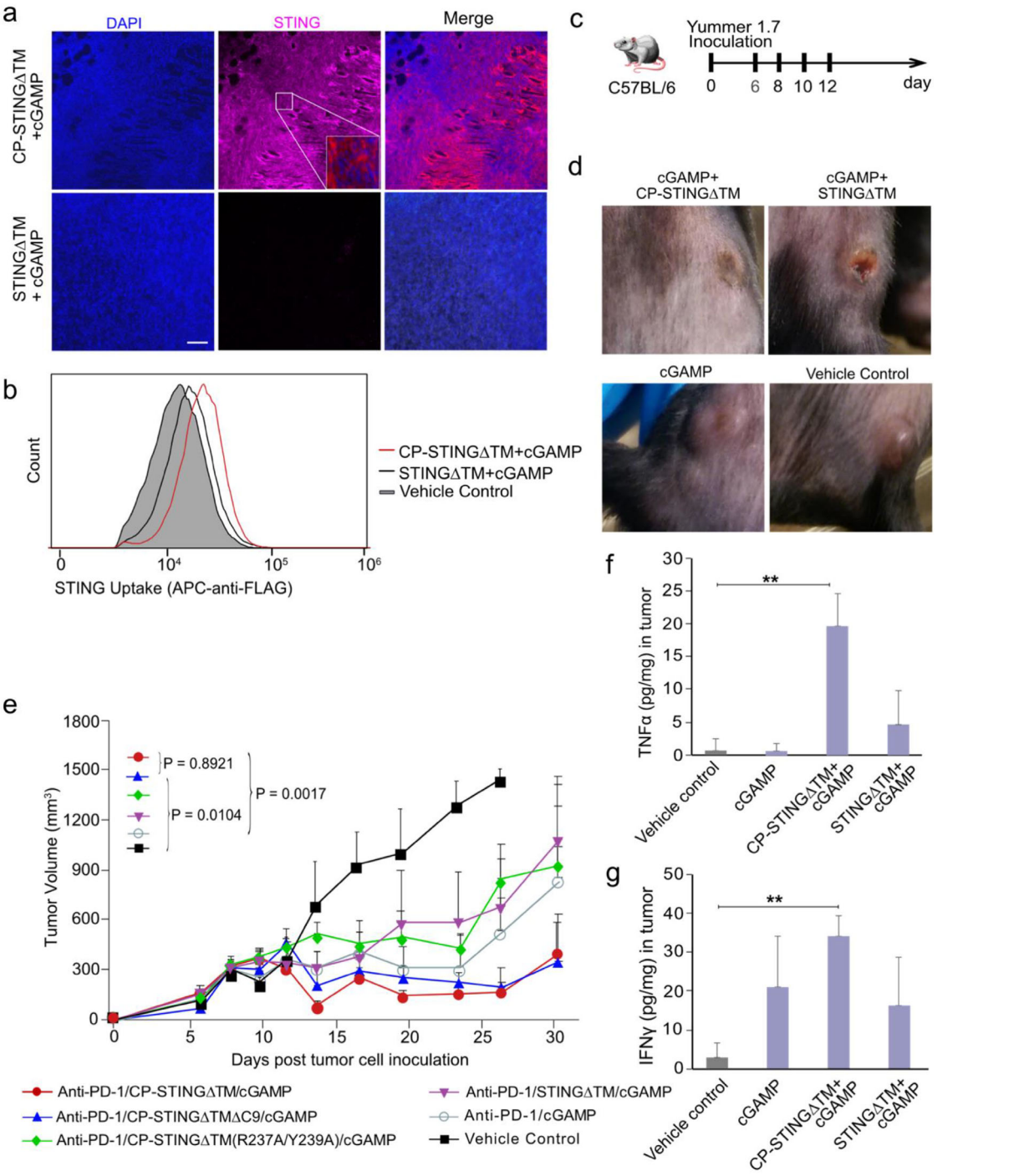

Figure 6. Combination of CP-STINGΔTM/cGAMP and anti-PD-1 in a syngeneic mouse melanoma model. Groups of C57BL/6 mice were inoculated with 1 million YUMMER1.7 melanoma cells in the right flank and when tumors reached 150–170 mm^3, "137.5 μg CP-STINGΔTM + 2.5 μg cGAMP," or "100 μg STINGΔTM + 2.5 μg cGAMP" were i.t. administered. After 96 h, cellular uptake of CP-STINGΔTM or STINGΔTM was analyzed by anti-FLAG staining for a) fluorescence microscopy (scale bar = 100 μm) and b) flow cytometry, respectively. Data are representative of two mice. c) Schematic of tumor treatment. Specifically, when tumors reached 150–170 mm^3, mice were treated with i.p. injection of anti-PD-1 (200 μg per mouse) and concurrently with i.t. injection of different STING variants every 2 d for a total of four injections: "137.5 μg CP-STINGΔTM + 2.5 μg cGAMP" ($n = 5$), "137.5 μg CP-STINGΔTMΔC9 + 2.5 μg cGAMP" ($n = 5$), "137.5 μg CP-STINGΔTM(R237A/Y239A) + 2.5 μg cGAMP" ($n = 5$), "100 μg STINGΔTM + 2.5 μg cGAMP" or "2.5 μg mL^{-1} cGAMP only" ($n = 5$), and vehicle control ($n = 4$). Different mass concentrations were adjusted to ensure 1:1 molar ratio between STING dimer and cGAMP. d) Photos for acute responses for the treatment were taken 72 h after treatment. e) Overall tumor growth curves were measured using clipper, and tumor volume was calculated using formulations $V = (L \times W \times W)/2$, where V is tumor volume, L is tumor length, and W is tumor width. f) TNF-α and g) IFN-γ were quantified by ELISA in tumors receiving indicated treatments ($n = 3$). Statistical analysis was performed by one-way ANOVA: $^*P < 0.05$, $^{**}P < 0.01$.

preclinical NSCLC mouse xenograft model as an anticancer therapy. Importantly, while the N terminus of Omomyc is responsible for cell targeting, the C terminus of STINGΔTM is involved in intracellular STING functions.[22] Additionally, the two protein domains exist as a dimer on their own. Therefore, the fusion protein consisting of CP and STINGΔTM can in theory function properly with the natural configuration and stoichiometry. To confirm the functionality and versatility of the fusion protein CP-STINGΔTM, we tested a panel of NSCLC and melanoma cancer cell lines since these two cancer types can benefit from existing immunotherapy owing to high tumor mutational burden. Intriguingly, we found that CP-STINGΔTM plays distinct roles in these cell lines depending on the levels of endogenous STING expression. Specifically, codelivery of CP-STINGΔTM and cGAMP restores the STING signaling in cancer cells either naturally deficient for STING expression or genetically knocked out by CRISPR, indicating that CP-STINGΔTM and cGAMP forms a functional complex in this setting. On the contrary, CP-STINGΔTM serves as a chaperon to markedly promote the delivery of cGAMP in cells with downregulated STING expression, requiring a 100-fold lower concentration of cGAMP than free cGAMP in STING activation and subsequent type I IFN induction.

To explore the potential translation of the platform, we further confirmed potent T cell proliferation and antitumor immune responses ex vivo and extended the observation in vivo using a mouse model of vaccination. Finally, we investigated the translational potential of our platform in combination with the ICB using a syngeneic mouse melanoma model. Intratumoral administration of CP-STINGΔTM and cGAMP was chosen because in contrast to conventional chemotherapy, local administration of immunotherapies can take advantage of the tumor itself as a rich source of neoantigens to amplify the immune responses locally to achieve systemic protection, and meanwhile avoiding potential systemic toxicities. This principle has been successfully applied in existing immune therapeutics, including but not limited to, immune cytokines, ICB and replicon RNA.[45,46] Collectively, our CP-STINGΔTM system may provide a new paradigm of delivering STING agonists toward vaccines and cancer immunotherapy.

The most important finding of our study is that CP-STINGΔTM in complex with cGAMP can form a functional complex to activate the endogenous STING signaling in cancer cells deficient for STING. This attribute may have critical clinical implications in melanoma and lung cancers. Notably, existing STING agonism strategies have centered around developing DNA-damaging reagents to activate tumor cells to produce endogenous cGAMP, reversing the epigenetic inhibition of STING/cGAS expression, and exogenously administering STING agonists. These approaches, however, can be hampered by the fact that endogenous STING and/or cGAS are frequently silenced in tumor cells as a mechanism to evade antitumor immune responses.[13] Specifically, the loss of tumor-intrinsic STING expression has been shown to impair tumor cell antigenicity and susceptibility to lysis by tumor-infiltrating lymphocytes through the downregulation of MHC class I expression on the surface of cancer cells. In addition to NSCLC and melanoma, decreased expression of STING in tumor cells has been correlated with poor prognosis in patients with gastric and colon cancers.[12,47] Conversely, activation of tumor-intrinsic STING signaling has been found to dictate chemotherapy-induced antitumor cytotoxic T cell responses (e.g., olaparib) in triple-negative breast cancer.[48,49]

In comparison to many existing nanomedicine and biomaterials for cancer immunotherapy,[50] one major departure of our protein-based strategy from the status quo is to tackle the essential problem of STING silencing in tumor cells. Existing nanomedicines and biomaterials for STING agonist delivery only administer the agonists to the TME and target innate immune cells and stroma cells with endogenous STING expression that existing methods does not solve the emerging clinical problem of STING silencing in tumor cells, which is critical for therapeutic responses. On the other hand, our protein-based technology in principle belongs to the class of biologics, such as immune cytokines (e.g., interleukin, IL-2, and IL-12) and ICB antibodies.[46,51,52] These protein-based therapeutics can be delivered in a vehicle free mode such as our cell-penetrating STING protein or in conjunction with nanomedicines and biomaterials, which have been used for delivery of immune cytokines. Additionally, our CP-STING protein as a delivery vehicle is unique in these aspects: 1) Instead of electrostatic complexation, which is particularly challenging to dinucleotides owing to low charge densities, we have made use of the inherent strong affinity between the C-terminus of STING and its agonist to efficiently encapsulate STING agonists. 2) The CP-STINGΔTM itself is in essence a single long polymer with a fixed degree of "polymerization" and therefore is structurally well defined as evidenced by size exclusion chromatography and SDS-PAGE. This feature may minimize batch-to-batch variations, commonly occurring in synthetic delivery vehicles. 3) The fusion protein can be produced and purified from the standard *E. coli* based recombinant protein expression system in a high yield in conjunction with the low-cost metal affinity purification, which is easily accessible to many laboratories. Future studies can involve comprehensive pharmacological characterization of the CP-STINGΔTM in the setting of systemic delivery to optimize the dose and frequency of the fusion protein. Additionally, by employing transgenic mouse models with STING deficiency in different cell types (e.g., tumor cells versus different immune cell subtypes), we can further elucidate exact targets of CP-STINGΔTM, and therefore assess the contribution of tumor-intrinsic STING in developing antitumor immune responses. Finally, given the modularity of the fusion protein, we can potentially substitute the cell-penetrating domain with a more specific protein domain such as nanobody to target particular cell type or TME such that our fusion platform can be extended to targeted delivery of STING agonists in a manner similar to antibody drug conjugates.[53] Alternatively, direction fusion of a nanobody such as anti-PD (L)1 with STINGΔTM may simultaneously leverage ICB and STING in a single protein format https://www.ncbi.nlm.nih.gov/pmc/articles/PMC7117931/. Therefore, our approach may offer a unique direction toward the STING-based therapeutics.

4. Experimental Section

Chemicals and Antibodies: 2'3'-cyclic-GMP-AMP (cGAMP) is a generous gift from Dr. Pingwei Li at Texas A&M University. Tween-20, Triton

X-100, and Triton X-114 were all purchased from Sigma-Aldrich (St Louis, MO). CFSE was purchased from Tonbo Biosciences (San Diego, CA). All other chemicals were purchased from ThermoFisher (Waltham, MA) and used as received. Human CXCL10/IP-10 and mouse CXCL10/IP-10 ELISA Kit, Murine TNF-α, and Murine IFN-γ were respectively purchased from R&D system (Minneapolis, MN) and Peprotech (Rocky Hill, NJ). Zombie Dyes, Alexa647 anti-DYKDDDDK Tag Antibody (Clone L5), APC antimouse CD8a (Clone 53–6.7), fluorescein isothiocyanate (FITC) antimouse CD3 (clone 145-2C11), PerCP-Cy5.5 antimouse CD4 (Clone 129.29), Phycoerythrin (PE) antimouse CD8a (clone 53–6.7), PerCP-Cy5.5 cd11b (Clone M1/70), FITC antimouse cd11c (Clone N418), PE antimouse CD45 (clone 30-F11), Alexa 488 antimouse CD45 (clone 30-F11), FITC antihuman human leukocyte antigen (HLA)-A,B,C Antibody (clone W6/32), FITC antimouse H-2Kb/H-2Db Antibody (Clone 26-8-6) were from Biolegend (San Diego, CA). Primary antibodies of STING/TM173 (D2P2F), alpha-Tubulin (DM1A), TBK1/NF-κB nuclear factor kappa light chain enhancer of activated B cells (NAK) activating kinase (D1B4) were from Cell signaling technology (CST, Danvers, MA). Secondary antibodies of goat antirabbit IgG-horseradish peroxidase (HRP) and goat antimouse IgG-HRP are from Santa Cruz Biotech (Santa Cruz, CA). InVivoMAb antimouse PD-1 (CD279) was purchased from BioXCell (Lebanon, NH).

Expression and Purification of STINGΔTM Protein Variants: The human STINGΔTM protein (139-379aa) and mouse STINGΔTM (138-378aa) variants were synthesized by gblock (Integrated DNA Technologies, Coralville, IA), and cloned into pSH200 vector (a generous gift from Prof. Xiling Shen at Duke University) containing a 6xhistidine tag (His-tag), between *NcoI* and *NotI* sites. Mutants were generated with site-specific mutagenesis based on the human STINGΔTM plasmids. All plasmids were confirmed by sequencing. STINGΔTM variants were expressed as His-tag proteins from BL21 (DE3) Escherichia coli (*E. coli*). All proteins were expressed as cultures grown in Luria-Bertani broth (5 g sodium chloride, 5 g tryptone, 2.5 g yeast extract, and 500 mL of distilled water), supplemented with 100 μg mL^{-1} Ampicillin. After outgrowth at 37 °C with 225 rpm in a shaker, and until optical density (OD600) reached 0.6 × 10^{-3} and 1 × 10^{-3} M Isopropyl β-D-1-thiogalactopyranoside (IPTG) was added to induce the protein expression for 16 to 18 h at 20 °C and 225 rpm. Cells were then collected by centrifugation at 5000 x *g* for 20 min at room temperature. The bacterial pellets were resuspended in a 10 mL protein binding buffer (50 × 10^{-3} M sodium phosphate, 0.5 M sodium chloride, 10 × 10^{-3} M imidazole) and stored at −80 °C until purification. The frozen cultures were thawed and lysed with 1% Triton-100, 1 mg mL^{-1} lysozyme, 1 × 10^{-3} M phenylmethylsulfonyl fluoride (PMSF), and one ethylenediaminetetraacetic acid (EDTA)-free protease inhibitor cocktail tablet at room temperature for 20 min. The lysate was disrupted by ultrasonication at 5-second intervals for a total of 5 min each at 18 W on ice. Insoluble debris was removed by centrifugation at 12 000 x *g* for 60 min, at 4 °C. Protein purification was carried out by affinity chromatography using Cobalt agarose beads. 10 mL of raw protein extracts were applied to the protein binding buffer-equilibrated beads, followed by three washes with protein binding buffer plus 0.1% Triton-114 for endotoxin removal. After elution (50 × 10^{-3} M sodium phosphate, 0.5 M sodium chloride, 150 × 10^{-3} M imidazole), protein extracts were loaded to fast protein liquid chromatography (NGC Quest 10 Chromatography System, Biorad) for 3X PBS buffer exchange and purification. Protein fractions detected at $\lambda = 280$ nm were collected. Purified STINGΔTM variants concentrations were determined by DC protein assay and purities were verified by SDS-PAGE. Protein aliquots were kept at −80 °C at all times until further use.

DLS: Desired proteins were mixed with free cGAMP at the theoretical 1:1 molar ratio in PBS. Complexes were incubated for 30 min before data acquisition. Hydrodynamic size and polydispersity index were measured using dynamic light scattering (Malvern ZS90 particle analyzer, $\lambda = 633$ nm). Data were acquired at room temperature.

Animal Work: All work with C57BL/6J mice (females, 7–10 weeks old) and OT-1 transgenic mice (The Jackson Laboratory, Bar Harbor, ME) was performed in accordance with institutional guidelines under protocols of NU-20-0312R (C57BL/6J) and NU-19-0106R (OT-1) approved by Northeastern University-Institutional Animal Care and Use Committee (NU-IACUC). All mice were maintained in a pathogen-free facility following the National Research Council of the National Academies.

Cell Lines and Cell Culture: Non-small cell lung cancer cell lines A549, H1944, and H2122 harboring KRAS/LKB1 comutations and H1944 Knockouts (H1944 STING-knockout, H1944 cGAS-knockout, H1944 scramble-knockout) were generous gifts from Dr. David Barbie's lab. RAW-Blue ISG cells and RAW-Blue were purchased from Invivogen (San Diego, CA, USA). B16F10, HeLa, HEK293T, SK-MEL-3, and SK-MEL-5, were obtained from the American Type Culture Collection (ATCC, Rockville, MD). Yummer1.7 was requested from the Koch Institute (Cambridge, MA). B16-OVA(257-264aa) and Yummer1.7-OVA(257-264aa) were generated through transfection with plasmids encoding full lengths of OVA and enhanced green fluorescent protein (EGFP), and sorted by fluorescence-activated cell sorting (FACS) for GFP expression. A549, SK-MEL-3, SK-MEL-5, Yummer1.7, HeLa, and HEK293T were cultured in Dulbecco's modified Eagle's medium (DMEM) supplemented with 10% fetal bovine serum (FBS), 100 U mL^{-1} penicillin-streptomycin, and 100x nonessential amino acid (NEAA). H1944, H2122, HCC44, and H23 were cultured in Roswell Park Memorial Institute Medium (RPMI)-1640 supplemented with 10% FBS, 100 U mL^{-1} penicillin-streptomycin, and 100x NEAA. H1944 STING-knockout, H1944 cGAS-knockout, and H1944 scramble-knockout were cultured in RPMI-1640, with 10% FBS, 100 U mL^{-1} penicillin-streptomycin, 100x NEAA with 1 μg mL^{-1} puromycin selection. Cells were kept in a humidified incubator with 5% carbon dioxide (CO_2) at 37 °C and routinely tested mycoplasma negative by polymerase chain reaction. All the cell experiments were performed between passages 2 and 10.

In Vitro STING Signaling Activation and Endotoxin Assays: RAW-Blue ISG cells (for the STING activation) or RAW-Blue (for endotoxin detection in OVA) were seeded in 96-well plates at 3 × 10^5 cells mL^{-1} in 100 μL DMEM with 10% heat inactivated FBS and 1% penicillin/streptomycin per well. After 24 h incubation, 5 μg STING ΔTM protein (or mutants) with 0.125 μg cGAMP premixed and equilibrated in 20 μL Opti-minimal essential medium (MEM) media was added to RAW-Blue ISG cells in each well and incubated overnight. Similarly, to check endotoxin contamination in OVA used for animal studies, OVA was added to RAW-Blue at 5 μg protein per well and incubated overnight. After incubation, 20 μL of the induced cell supernatant was added to 180 μL QUANTI-Blue solution per well of a 96-well plate. The plate was incubated in 37 °C for 30 min–10 h until a visible color difference was observed. IFN-secreted embryonic alkaline phosphatase activity was then determined by the absorbance at 650 nm with a spectrophotometer.

Lentivirus Production and Cell Line Generation: Lentiviral vector plasmids of *pFUW Ubc OVA (252-271aa) EGFP, EGFP Luciferase puro (663)* were used to generate lentiviral particles. 7.5 μg of packaging plasmid psPAX2, 2.5 μg of envelope plasmid pMD2.G, 10 μg of Lentiviral vector plasmids, and 10 μL TransIT-X2 were mixed in 1 mL Opti-MEM. After 30 min of incubation at room temperature, the plasmid mixture was added to 70% confluency HEK293T cells. Supernatants were collected at 48 and 72 h after transfection and centrifuged at 1000 g for 10 min to remove the debris. Harvested Lenti-viral supernatants were kept at −80 °C until further cell line generation. After targeted cell lines of B16F10 and Yummer 1.7 reached 70% confluency, lentiviral supernatants were added to the cells with 8 μg mL^{-1} polybrene. Transfected cells were selected with 1 μg mL^{-1} puromycin.

ELISA: For human CXCL10 and mouse CXCL10, cells (1–2 × 10^4) were cultured with premixed complexes of 40 μg mL^{-1}, or 10 μg mL^{-1} STINGΔTM variants with or without 1 or 0.25 μg mL^{-1} cGAMP for 72 h. Conditioned supernatants were collected for ELISA quantification according to the manufacturer's instructions. Values represent the average of four to six replicates from at least two independent experiments. For analysis of anti-OVA IgG level, the ELISA was conducted as previously described.[15] For cytokine quantification in the treatment study, tumors were harvested and grounded in tissue protein extraction reagent (T-PER) with 1% proteinase inhibitors. The lysates were incubated at 4 °C for 30 min with rotation. The supernatant from each lysate was collected after removing debris through centrifugation. The quantifications of CXCL10, TNF-α, and IFN-γ were performed according to the manufacturer's instructions.

Immunofluorescence Staining: A549, H1944, and HeLa were seeded in chamber slides at a density of ≈5×10^4 24 h before incubation with 40 μg mL^{-1} STINGΔTM variants and 1 μg mL^{-1} cGAMP complexes. After another 24 h, cells were washed with PBS once, and fixed with 70% ethanol. After permeabilization with PBS containing 0.1% Triton X-100 for 15 min, cells were washed and incubated with the anti-DYKDDDDK Tag antibody at 1:500 dilution in 1x PBS with 1% bovine serum albumin (BSA) and 0.05% polyethylene glycol sorbitan monolaurate solution (TWEEN) 20 (PBST) at 4 °C overnight. Cells were then washed for 30 min in PBST and incubated with Alexa488-Phalloidin (CST) in 1:100 dilution for 1 h. After washing cells with PBST for three times for 10 min each, cells were counter-stained with 4′,6-diamidino-2-phenylindole (DAPI) in mounting media at room temperature. Images of the cells were visualized and captured by Nikon Eclipse Ti2 microscope (Tokyo, Japan) and analyzed by ImageJ National Institutes of Health.

Fluorescence Imaging Analysis: Three days after injection with complexes, tumors were harvested and placed in optimal cutting temperature (OCT) compound in tissue cassettes and frozen on ice for cutting into 8—10 μm sections in slides. The slides were washed with PBS for 10 min at room temperature, dried on a paper towel and incubated with anti-CD45 diluted in the antibody buffer (10% FBS in PBS) for 1 h at room temperature in the dark. After three washes with PBS, the slides were fixed in 4% paraformaldehyde in PBS. Slides were incubated with 0.025% saponin in PBS for permeabilization. Anti-DYKDDDDK were added on the sections for overnight incubation at 4 °C in the dark. Slides were washed in PBS with 0.0025% saponin for 10 min twice. After incubating with secondary antibody for 1 h in the dark, slides were rinsed with PBS with 0.0025% saponin and counterstained with DAPI. The stained tumor slides were imaged using a Nikon microscope.

Flow Cytometry: For uptake study, 1×10^5 cells were seeded in 12-well plates in their corresponding complete culture medium and incubated for 24 h. After treatment with 40 μg mL^{-1} STINGΔTM variants with or without 1 μg mL^{-1} cGAMP for 24 h, cells were washed with PBS and treated with trypsin for at least 15 min to remove STING proteins nonspecifically bound to the cell surface. Cells were transferred to 96-well v-bottom plates and collected through 300 x *g* centrifugation for 3 min. After twice washes with 200 μL PBS, cells were fixed with 70% ethanol for 20 min. The fixed cells were washed with PBS for 10 min three times. Cells were resuspended in anti-DYKDDDDK Tag Antibody at 1:1000 dilution in antibody dilution buffer (1x PBS containing 1% BSA and 0.05% Tween 20) and incubated for 2 h at room temperature in the dark. Antibodies were removed by rinsing cells with PBST three times. The cell suspension in PBS was loaded to Attune flow cytometry (Thermofisher, Waltham, MA). Doublets and dead cells were excluded before analysis.

For in vitro MHC-I analysis, 10 000 cells were incubated with 40 μg mL^{-1} STINGΔTM variants and 1 μg mL^{-1} cGAMP in a complete culture medium for 48 h before staining. Cells were rinsed by PBS, detached by 100 μL 5×10^{-3} M EDTA in PBS with a fixable live/dead dye, NIR Zombie Dye (Biolegend), at 1:1000 dilution for dead cell exclusion. After staining was quenched by FACS buffer (5% FBS, 2×10^{-3} M EDTA, 0.1% sodium azide in PBS), cells were resuspended by FACS buffer containing 0.4 μg mL^{-1} antihuman HLA-A,B,C antibody or FITC antimouse H-2Kb/H-2Db antibody, and incubated on ice for 30 min in the dark. Stained cells were washed twice and resuspended in the FACS buffer for flow cytometric analysis in FlowJo (Franklin Lakes, NJ). After excluding doublets and debris of dead cells, gating strategies determined through control staining were applied for analysis while compared with FITC Mouse IgG2a, κ Isotype control antibody stained cells.

For OT-1 CD8+ T cells stimulation, CFSE stained lymphocytes were collected through 500 x *g* centrifuge for 3 min and washed with 200 μL PBS. 100 μL Zombie dye in PBS at 1:1000 dilution was added to the lymphocyte and incubated for 30 min at room temperature avoiding light. Zombie dye staining was quenched by 100 μL FACS buffer. After 3 min centrifuge at 500 x g, OT-1 CD8$^+$ T cells were selected by 100 μL APC antimouse CD8a Antibody in FACS buffer at 1:1000 dilution after 30 min incubation on ice. Costained cells were resuspended in the FACS buffer and quantified under the flow cytometer.

For in vivo tumor profiling, dissected tumors were digested in 1 mg mL^{-1} collagenase D for 1 h at 37 °C. Single-cell suspensions were obtained from mincing the tumor through a 70 μm cell strainer. After staining with NIR zombie dye for dead cell exclusion, cells were neutralized and blocked with anti-CD16/CD32 for 5 min on ice and stained with antibodies against surface markers CD45, CD3, CD4, CD8, CD11b, CD11c on ice for 30 min in FACS buffer. For intracellular staining, cells were fixed, permeabilized, and stained with anti-DYKDDDDK tag antibody. All samples were analyzed by FlowJo after loading to the flow cytometer.

Cell Viability Assay: The effects of STINGΔTM variants and cGAMP complexes on cell viability were determined by MTT assay. 1000 cells were seeded in 96-well plates and treated with 40 μg mL^{-1} STINGΔTM variants and 1 μg mL^{-1} cGAMP for 120 h in 5% CO_2 at 37 °C in a humidified incubator. Cells were further incubated with 0.5 mg mL^{-1} MTT dissolved in sterilized 1x PBS at 37 °C for 2 h before dimethyl sulfoxide was added into each well to dissolve formazan crystals. The absorbance of each well was determined at 570 nm on an automated Bio-Rad microplate reader (Bio-Rad Laboratories, Hercules, CA). Untreated cells as control were considered to be 100% viable.

Lymphocyte Preparation from Lymph Nodes in OT-1 Mice: The mesenteric, inguinal, axillary, and brachial lymph nodes dissected from OT-1 mouse were homogenized to generate a single cell suspension and the released cells in lymphocyte growth medium (RPMI1640 complete media and 50×10^{-6} M 2-mercaptoethanol) were pelleted and resuspended in 10 mL PBS. The lymphocyte was washed and stained with 1×10^{-6} M CFSE in 1x PBS for 20 min until the staining was terminated by 10% FBS. The stained lymphocyte was resuspended and cultured in lymphocyte growth medium in a humidified incubator to release excessive CFSE. After 2 h incubation, lymphocyte was collected and resuspended in lymphocyte growth medium with 20 U mL^{-1} IL-2.

Coculture of OT1 Lymphocytes with B16-OVA or YUMMER 1.7-OVA: 100 μL of 1×10^6 lymphocytes in lymphocyte growth medium with 20 U mL^{-1} IL-2 was added into the 96-well plate with 100 μL of 1×10^4 B16-OVA(257-264aa) treated with STINGΔTM variants with or without cGAMP 48 h ahead. On days 3, 100 μL of lymphocytes were gently collected for flow cytometry analysis. 100 μL fresh lymphocyte growth medium with 20 U mL^{-1} IL-2 was added to each well for leftover lymphocyte growth. On day 5, after lymphocytes were collected, B16-OVA(257-264aa) attached wells were washed with PBS twice for subsequent MTT assay.

Immunizations, Tumor Inoculation, and Treatment in Mice: Analysis of immunizations for adjuvant potential performed in C56BL/6 mice with B16-OVA (257-264aa) was conducted as previously described.[15] For treatment study, one million Yummer1.7 cells in 100 μL Opti-MEM were subcutaneously injected into the flank of mice. At 6–9 d later, when tumors reached 150 mm^3 in volume, animals were injected intratumorally with ≈25 μL vehicle control, 2.5 μg cGAMP only or 100 μg STINGΔTM variants and 2.5 μg cGAMP complex in Opti-MEM.

Statistical Analysis: Statistical significance was evaluated using one-way ANOVA followed by Tukey post hoc test. *P* values less than 0.05 were considered significant. Statistical significance is indicated in all figures according to the following scale: $*P < 0.05$, $**P < 0.01$, $***P < 0.001$, and $****P < 0.0001$. All graphs are expressed as the means ± SEM. In one-way ANOVA followed by post hoc tests, asterisks were marked only in pairs of the interest.

Supporting Information

Supporting Information is available from the Wiley Online Library or from the author.

Acknowledgements

This work was supported by the Northeastern University Faculty start-up funding (J.L.), Northeastern University-Dana Farber Cancer Institute

Cancer Drug Development (J.L. and D.A.B.), and Peer Reviewed Medical Research Program from the Department of Defense's Congressionally Directed Medical Research Programs (J.L.). The authors are grateful to Dr. Yingzhong Li at the Koch Institute of Integrative Cancer Research at Massachusetts Institute of Technology for scientific advice. The authors would like to express their gratitude to Professor Sara Rouhanifard at Northeastern University's Department of Bioengineering for generously sharing her lab's fluorescent microscope and Professor Ke Zhang at Northeastern University's Department of Chemistry for sharing his lab's equipment.

Conflict of Interest

A U.S. Provisional Application No.: 62/979733 has been filed by Northeastern University for the invention.

Data Availability Statement

Data sharing is not applicable to this article as no new data were created or analyzed in this study.

Keywords

cyclic dinucleotides, STING, vaccine and immunotherapy

Received: March 10, 2021
Revised: May 16, 2021
Published online: June 20, 2021

[1] J. Ahn, G. N. Barber, *Exp. Mol. Med.* **2019**, *51*, 1.
[2] A. J. Pollock, S. A. Zaver, J. J. Woodward, *Nat. Commun.* **2020**, *11*, 3533.
[3] J. Kwon, S. F. Bakhoum, *Cancer Discovery* **2020**, *10*, 26.
[4] J. M. Ramanjulu, G. S. Pesiridis, J. Yang, N. Concha, R. Singhaus, S.-Y. Zhang, J.-L. Tran, P. Moore, S. Lehmann, H. C. Eberl, M. Muelbaier, J. L. Schneck, J. Clemens, M. Adam, J. Mehlmann, J. Romano, A. Morales, J. Kang, L. Leister, T. L. Graybill, A. K. Charnley, G. Ye, N. Nevins, K. Behnia, A. I. Wolf, V. Kasparcova, K. Nurse, L. Wang, A. C. Puhl, Y. Li, M. Klein, C. B. Hopson, J. Guss, M. Bantscheff, G. Bergamini, M. A. Reilly, Y. Lian, K. J. Duffy, J. Adams, K. P. Foley, P. J. Gough, R. W. Marquis, J. Smothers, A. Hoos, J. Bertin, *Nature* **2018**, *564*, 439.
[5] L. Corrales, L. H. Glickman, S. M. McWhirter, D. B. Kanne, K. E. Sivick, G. E. Katibah, S.-R. Woo, E. Lemmens, T. Banda, J. J. Leong, K. Metchette, T. W. Dubensky, T. F. Gajewski, *Cell Rep.* **2015**, *11*, 1018.
[6] M. C. Hanson, M. P. Crespo, W. Abraham, K. D. Moynihan, G. L. Szeto, S. H. Chen, M. B. Melo, S. Mueller, D. J. Irvine, *J. Clin. Invest.* **2015**, *125*, 2532.
[7] D. Shae, K. W. Becker, P. Christov, D. S. Yun, A. K. R. Lytton-Jean, S. Sevimli, M. Ascano, M. Kelley, D. B. Johnson, J. M. Balko, J. T. Wilson, *Nat. Nanotechnol.* **2019**, *14*, 269.
[8] L. Li, Q. Yin, P. Kuss, Z. Maliga, J. L. Millán, H. Wu, T. J. Mitchison, *Nat. Chem. Biol.* **2014**, *10*, 1043.
[9] X. Lu, L. Miao, W. Gao, Z. Chen, K. J. McHugh, Y. Sun, Z. Tochka, S. Tomasic, K. Sadtler, A. Hyacinthe, Y. Huang, T. Graf, Q. Hu, M. Sarmadi, R. Langer, D. G. Anderson, A. Jaklenec, *Sci. Transl. Med.* **2020**, *12*, eaaz6606.
[10] K. S. Park, C. Xu, X. Sun, C. Louttit, J. J. Moon, *Adv. Ther.* **2020**, *3*, 2000130.
[11] M. Wehbe, L. Wang-Bishop, K. W. Becker, D. Shae, J. J. Baljon, X. He, P. Christov, K. L. Boyd, J. M. Balko, J. T. Wilson, *J. Controlled Release* **2020**, *330*, 1118.
[12] T. Xia, H. Konno, J. Ahn, G. N. Barber, *Cell Rep.* **2016**, *14*, 282.
[13] G. N. Barber, *Nat. Rev. Immunol.* **2015**, *15*, 760.
[14] S. Kitajima, E. Ivanova, S. Guo, R. Yoshida, M. Campisi, S. K. Sundararaman, S. Tange, Y. Mitsuishi, T. C. Thai, S. Masuda, B. P. Piel, L. M. Sholl, P. T. Kirschmeier, C. P. Paweletz, H. Watanabe, M. Yajima, D. A. Barbie, *Cancer Discovery.* **2019**, *9*, 34.
[15] Y. He, C. Hong, E. Z. Yan, S. J. Fletcher, G. Zhu, M. Yang, Y. Li, X. Sun, D. J. Irvine, J. Li, P. T. Hammond, *Sci. Adv.* **2020**, *6*, eaba7589.
[16] M.-E. Beaulieu, T. Jauset, D. Massó-Vallés, S. Martínez-Martín, P. Rahl, L. Maltais, M. F. Zacarias-Fluck, S. Casacuberta-Serra, E. S. del Pozo, C. Fiore, L. Foradada, V. C. Cano, M. Hervás, M. Guenther, E. R. Sanz, M. Oteo, C. Tremblay, G. Martín, D. Letourneau, M. Montagne, M. Á. M. Alonso, J. R. Whitfield, P. Lavigne, L. Soucek, *Sci. Transl. Med.* **2019**, *11*, eaar5012.
[17] R. D. Junkins, M. D. Gallovic, B. M. Johnson, M. A. Collier, R. Watkins-Schulz, N. Cheng, C. N. David, C. E. McGee, G. D. Sempowski, I. Shterev, K. McKinnon, E. M. Bachelder, K. M. Ainslie, J. P.-Y. Ting, *J. Controlled Release* **2018**, *270*, 1.
[18] L. Wang-Bishop, M. Wehbe, D. Shae, J. James, B. C. Hacker, K. Garland, P. P. Chistov, M. Rafat, J. M. Balko, J. T. Wilson, *J. Immunother. Cancer* **2020**, *8*, e000282.
[19] S. A. Patel, A. J. Minn, *Immunity* **2018**, *48*, 417.
[20] S. L. Ergun, D. Fernandez, T. M. Weiss, L. Li, *Cell* **2019**, *178*, 290.
[21] S. L. Ergun, L. Li, *Trends Cell Biol.* **2020**, *30*, 399.
[22] Y. Tanaka, Z. J. Chen, *Sci. Signaling* **2012**, *5*, ra20.
[23] B. Zhao, F. Du, P. Xu, C. Shu, B. Sankaran, S. L. Bell, M. Liu, Y. Lei, X. Gao, X. Fu, F. Zhu, Y. Liu, A. D. Laganowsky, X. Zheng, J. Ji, A. P. West, R. O. Watson, P. Li, *Nature* **2019**, *569*, 718.
[24] C. Zhang, G. Shang, X. Gui, X. Zhang, X. Bai, Z. J. Chen, *Nature* **2019**, *567*, 394.
[25] X. Zhang, H. Shi, J. Wu, X. Zhang, L. Sun, C. Chen, Z. J. Chen, *Mol. Cell* **2013**, *51*, 226.
[26] G. Shang, C. Zhang, Z. J. Chen, X. Bai, X. Zhang, *Nature* **2019**, *567*, 389.
[27] Y.-H. Huang, X.-Y. Liu, X.-X. Du, Z.-F. Jiang, X.-D. Su, *Nat. Struct. Mol. Biol.* **2012**, *19*, 728.
[28] S. Ouyang, X. Song, Y. Wang, H. Ru, N. Shaw, Y. Jiang, F. Niu, Y. Zhu, W. Qiu, K. Parvatiyar, Y. Li, R. Zhang, G. Cheng, Z.-J. Liu, *Immunity* **2012**, *36*, 1073.
[29] C. Shu, G. Yi, T. Watts, C. C. Kao, P. Li, *Nat. Struct. Mol. Biol.* **2012**, *19*, 722.
[30] M. J. Demma, C. Mapelli, A. Sun, S. Bodea, B. Ruprecht, S. Javaid, D. Wiswell, E. Muise, S. Chen, J. Zelina, F. Orvieto, A. Santoprete, S. Altezza, F. Tucci, E. Escandon, B. Hall, K. Ray, A. Walji, J. O'Neil, *Mol. Cell. Biol.* **2019**, *22*, e00248.
[31] G. Preta, J. G. Cronin, I. M. Sheldon, *Cell Commun. Signaling* **2015**, *13*, 24.
[32] A. Sistigu, T. Yamazaki, E. Vacchelli, K. Chaba, D. P. Enot, J. Adam, I. Vitale, A. Goubar, E. E. Baracco, C. Remédios, L. Fend, D. Hannani, L. Aymeric, Y. Ma, M. Niso-Santano, O. Kepp, J. L. Schultze, T. Tüting, F. Belardelli, L. Bracci, V. L. Sorsa, G. Ziccheddu, P. Sestili, F. Urbani, M. Delorenzi, M. Lacroix-Triki, V. Quidville, R. Conforti, J.-P. Spano, L. Pusztai, V. Poirier-Colame, S. Delaloge, F. Penault-Llorca, S. Ladoire, L. Arnould, J. Cyrta, M. C. Dessoliers, A. Eggermont, M. E. Bianchi, M. Pittet, C. Engblom, C. Pfirschke, X. Préville, G. Uzè, R. D. Schreiber, M. T. Chow, M. J. Smyth, E. Proietti, F. André, G. Kroemer, L. Zitvogel, *Nat. Med.* **2014**, *20*, 1301.
[33] L. Galluzzi, A. Buqué, O. Kepp, L. Zitvogel, G. Kroemer, *Nat. Rev. Immunol.* **2017**, *17*, 97.
[34] R. Falahat, P. Perez-Villarroel, A. W. Mailloux, G. Zhu, S. Pilon-Thomas, G. N. Barber, J. J. Mulé, *Cancer Immunol. Res.* **2019**, *7*, 1837.
[35] V. K. Gonugunta, T. Sakai, V. Pokatayev, K. Yang, J. Wu, N. Dobbs, N. Yan, *Cell Rep.* **2017**, *21*, 3234.
[36] T. Xia, H. Konno, G. N. Barber, *Cancer Res.* **2016**, *76*, 6747.

[37] T. Li, Z. J. Chen, *J. Exp. Med.* **2018**, *215*, 1287.
[38] J. Wang, P. Li, M. X. wu, *J. Invest. Dermatol.* **2016**, *136*, 2183.
[39] J. Fu, D. B. Kanne, M. Leong, L. H. Glickman, S. M. McWhirter, E. Lemmens, K. Mechette, J. J. Leong, P. Lauer, W. Liu, K. E. Sivick, Q. Zeng, K. C. Soares, L. Zheng, D. A. Portnoy, J. J. Woodward, D. M. Pardoll, T. W. Dubensky, Y. Kim, *Sci. Transl. Med.* **2015**, *7*, 283ra52.
[40] J. Volckmar, L. Knop, S. Stegemann-Koniszewski, K. Schulze, T. Ebensen, C. A. Guzmán, D. Bruder, *Vaccine* **2019**, *37*, 4963.
[41] S. Budhu, D. A. Schaer, Y. Li, R. Toledo-Crow, K. Panageas, X. Yang, H. Zhong, A. N. Houghton, S. C. Silverstein, T. Merghoub, J. D. Wolchok, *Sci. Signaling* **2017**, *10*, eaak9702.
[42] J. Wang, C. J. Perry, K. Meeth, D. Thakral, W. Damsky, G. Micevic, S. Kaech, K. Blenman, M. Bosenberg, *Pigm. Cell Melanoma Res.* **2017**, *30*, 428.
[43] Q. Jin, W. Zhu, J. Zhu, J. Zhu, J. Shen, Z. Liu, Y. Yang, Q. Chen, *Adv. Mater.* **2021**, *33*, 2007557.
[44] Q. Duan, H. Zhang, J. Zheng, L. Zhang, *Trends Cancer* **2020**, *6*, 605.
[45] Y. Li, Z. Su, W. Zhao, X. Zhang, N. Momin, C. Zhang, K. D. Wittrup, Y. Dong, D. J. Irvine, R. Weiss, *Nat. Cancer* **2020**, *1*, 882.
[46] N. Momin, N. K. Mehta, N. R. Bennett, L. Ma, J. R. Palmeri, M. M. Chinn, E. A. Lutz, B. Kang, D. J. Irvine, S. Spranger, K. D. Wittrup, *Sci. Transl. Med.* **2019**, *11*, eaaw2614.
[47] S. Song, P. Peng, Z. Tang, J. Zhao, W. Wu, H. Li, M. Shao, L. Li, C. Yang, F. Duan, M. Zhang, J. Zhang, H. Wu, C. Li, X. Wang, H. Wang, Y. Ruan, J. Gu, *Sci. Rep.* **2017**, *7*, 39858.
[48] J. L. Ritter, Z. Zhu, T. C. Thai, N. R. Mahadevan, P. Mertins, E. H. Knelson, B. P. Piel, S. Han, J. D. Jaffe, S. A. Carr, D. A. Barbie, T. U. Barbie, *Cancer Res.* **2020**, *80*, 44.
[49] C. Pantelidou, O. Sonzogni, M. D. O. Taveira, A. K. Mehta, A. Kothari, D. Wang, T. Visal, M. K. Li, J. Pinto, J. A. Castrillon, E. M. Cheney, P. Bouwman, J. Jonkers, S. Rottenberg, J. L. Guerriero, G. M. Wulf, G. I. Shapiro, *Cancer Discovery* **2019**, *9*, 722.
[50] Y. Shi, *Adv. Ther.* **2020**, *3*, 1900215.
[51] D. M. Francis, M. P. Manspeaker, A. Schudel, L. F. Sestito, M. J. O'Melia, H. T. Kissick, B. P. Pollack, E. K. Waller, S. N. Thomas, *Sci. Transl. Med.* **2020**, *12*, eaay3575.
[52] M. Dougan, J. R. Ingram, H.-J. Jeong, M. M. Mosaheb, P. T. Bruck, L. Ali, N. Pishesha, O. Blomberg, P. M. Tyler, M. M. Servos, M. Rashidian, Q.-D. Nguyen, U. H. von Andrian, H. L. Ploegh, S. K. Dougan, *Cancer Immunol. Res.* **2018**, *6*, 389.
[53] Y. J. Xie, M. Dougan, N. Jailkhani, J. Ingram, T. Fang, L. Kummer, N. Momin, N. Pishesha, S. Rickelt, R. O. Hynes, H. Ploegh, *Proc. Natl. Acad. Sci. USA* **2019**, *116*, 7624.

